Journal of Colloid and Interface Science 340 (2009) 218–224

Contents lists available at ScienceDirect

Journal of Colloid and Interface Science

www.elsevier.com/locate/jcis

A thermodynamic solution model for calcium carbonate: Towards an understanding of multi-equilibria precipitation pathways

Marcel Donnet, Paul Bowen *, Jacques Lemaître

Powder Technology Laboratory, Materials Institute, Station 12, Ecole Polytechnique Federale de Lausanne (EPFL), CH-1015 Lausanne, Switzerland

ARTICLE INFO

Article history:
Received 11 May 2009
Accepted 3 September 2009
Available online 9 September 2009

Keywords:
Calcium carbonate
Solubility
Interfacial energy
Surface potential
Crystal size
Reaction pathway

ABSTRACT

Thermodynamic solubility calculations are normally only related to thermodynamic equilibria in solution. In this paper, we extend the use of such solubility calculations to help elucidate possible precipitation reaction pathways during the entire reaction. We also estimate the interfacial energy of particles using only solubility data by a modification of Mersmann's approach. We have carried this out by considering precipitation reactions as a succession of small quasi-equilibrium states. Thus possible equilibrium precipitation pathways can be evaluated by calculating the evolution of surface charge, particle size and/or interfacial energy during the ongoing reaction. The approach includes the use of the Kelvin's law to express the influence of particle size on the solubility constant of precipitates, the use of Nernst's law to calculate surface potentials from solubility calculations and relate this to experimentally measured zeta potentials. Calcium carbonate precipitation and zeta potential measurements of well characterised high purity calcite have been used as a model system to validate the calculated values. The clarification of the change in zeta potential on titration illustrates the power of this approach as a tool for reaction pathway prediction and hence knowledge based tailoring of precipitation reactions.

1. Introduction

Supersaturation is the thermodynamic driving force for the formation of a solid phase by precipitation from an aqueous solution. The chemical composition of a solution is the main factor that determines its degree of supersaturation with respect to a given solid phase. Consequently the exact knowledge of this parameter is of great interest to control a precipitation reaction. Precipitation is often carried out by mixing two solutions to create a supersaturation with respect to a solid phase e.g. calcium nitrate and sodium carbonate to precipitate calcium carbonate. The degree of supersaturation produced on mixing the solutions has a major influence on the nucleation rate and subsequent crystal growth rate. The different crystal growth mechanisms and growth rates, such as screw dislocation or polysurface nucleation, depend on the suspersaturation and have different functional relationships. Also during the crystal growth and possible agglomeration mechanisms, the evolution of the chemical composition of the solution plays a key role by modifying the surface charges or the interfacial energy of the crystal. Interfacial energy is the sum of free energy of all the molecules present in the interface between different materials. The interface between a liquid and a gas is designated as the surface and the corresponding energy from this region is the surface energy or surface tension at the interface. For a solid–liquid or solid–solid interface the more general term interfacial energy is preferred. For a deeper understanding of the interaction between the solution chemistry and the interfacial energy, two different models are generally proposed [1–3]. The classical approach relates the induction time for nucleation for a specific precipitation reaction to the interfacial energy using experimental data [2]. One of the limitations of this approach is that crystal solution interfacial energies are only evaluated for the early stages of reaction. The second approach [1] is based on the chemical potential equilibrium between the solution, interface and crystal. This leads to a simple relationship between the concentrations of the species in solution and the interfacial energy of the ionic crystal under investigation. This approach can account for changes in interfacial energy as a function of the degree of precipitation. However the approach does not take into account species in solution other than the ion pair making up the ionic crystal. In the case of the surface charge, the interaction between the solid surface and the solution chemistry can be modelled by the Nernst concept of the potential determining ions. In order to use properly these models, the knowledge of the exact solution composition is required.

Such a precise knowledge of the solution composition is generally achieved using solubility calculations [4,5] because experimental characterisation is complex, difficult and time consuming. The calculation methods are based on thermodynamic equilibria of all species in the solution, including the activity correction in or-

* Corresponding author. Fax: +41 21 693 30 89.
E-mail address: paul.bowen@epfl.ch (P. Bowen).

0021-9797/$ - see front matter © 2009 Elsevier Inc. All rights reserved.
doi:10.1016/j.jcis.2009.09.005

Nomenclature

Symbol	Description (dimensions)
A	interface area (m^2)
A_D	debye coefficient ($L^{1/2}$ $K^{3/2}/mol^{3/2}$)
a_0	crystal lattice parameter (m)
B_D	Debye coefficient ($L^{1/2}K^{1/2}$/nm $mol^{1/2}$)
C	interface curvature (m)
C_0	correction coefficient of the ζ for ion adsorption in the Stern layer. (–)
$c_{i,S}, c_{j,S}$	analytical concentration of i (solute) or j (solvent) in the solid. (mol/m^3)
$c_{i,L}, c_{j,L}$	analytical concentration of i (solute) or j (solvent) in the liquid (mol/m^3)
f_i	activity coefficient of species i (–)
ΔG	Gibbs free energy change (J/mol)
I	ionic strength (mol/m^3)
I^*	ionic strength (mol/L)
K_S	solubility constant ($(mol/L)^{\nu}$)
M_r	molar solubility of particles with characteristic size r (mol/L)
M_0	molar solubility of infinite size particles (mol/L)
n	number of exchanged electrons (–)
M_W	molar weight (g/mol)
r	particle characteristic size (nm)
r_i	congestion radius of ion i (nm)
S	supersaturation (–)
S_{BET}	specific surface area as measured by the nitrogen adsorption (BET adsorption model) (m^2/g)
T	temperature (K)
V	volume (m^3)
[X]	concentration of dissolved species X (mol/L)
(X)	activity of dissolved species X (mol/L)
{X}	total analytical concentration of dissolved species X (mol/L)
z	valence of a $(z:z)$ electrolyte (–)

Constants

ε_0	permitivity of a vacuum (=8.8542 $\times$ 10^{-12}) (A s/V m)
F	Faraday constant (=96485) (C/mol)
k_B	Boltzmann's constant (=1.3807 $\times$ 10^{-23}) (J/K)
$N_{A\nu}$	Avogadro's number (=6.022 $\times$ 10^{23}) (1/mol)
R	Gas constant (=8.3144) (J/mol K)

Greek symbols

γ	interfacial energy (N/m)
ε_r	dielectric constant (–)
ε_0	permitivity of a vacuum (=8.8542 $\times$ 10^{-12}) (A s/V m)
κ	reciprocal Debye distance (1/m)
ρ	density (g/cm^3)
σ	surface charge density (C/m^2)
σ_{max}	maximum surface charge density (C/m^2)
ξ	reaction progress (–)
Φ_0	surface potential (V)
Φ_s	surface potential at Stern layer (V)
ψ	correction factor – zeta potential (–)
ζ	zeta potential: potential at particle-solvent shear plane (V)

der to approach their exact composition. More often than not, solubility calculations are only applied to calculate new dissociation constants [6–10] or initial solution compositions [11–17]. Thus, solubility calculations are only applied in general to equilibrated systems.

Our approach presented in this article is to apply solubility calculations to chemically non-equilibrated systems in order to account for precipitation reactions during the entire pathway. Also by combining solubility calculations with interfacial energy or surface charge evaluations, we aim to increase the reliability of these models with respect to experimental data. The approach allows direct comparison with precipitation reactions by following simple parameters such a pH which can be both calculated and measured experimentally, which has been rarely studied in the literature before. This paper also intends to extend the application field of solubility calculations in order to help the understanding of precipitation reaction pathways by considering pseudo equilibrium states at different degrees of reaction. By combining the solubility calculations with interfacial energy and surface charge evaluation, subtle differences between growth pathways can be tested which are otherwise difficult to measure in situ during reaction. The model systems used here for validation were the calcium carbonate precipitation reaction because of the significant quantity of data available in the literature and experimental evaluation of zeta potentials under well controlled conditions on high purity calcite powders.

2. Materials and methods

2.1. Materials

For the calculated interfacial energy, values encountered in the literature are not reliable so that we needed to carry out some complementary experiments. For these experiments, calcium carbonate powder is equilibrated under magnetic stirring conditions during 3 h in aqueous solutions (ultrapure water, conductivity of 0.055 μS/m and 0.02μm filtered) containing either 40.3 mM or 4.03 mM potassium carbonate (Merck 1.04928). These potassium carbonate solutions were prepared directly before the experiment and titrated with a standard acid solution. This protocol is used to minimise the amount of dissolved carbonic gas in the solution (<0.2% of the total added carbonate). The powder used for solution equilibration is either a low specific surface area calcite (Fluka, 21060, $S_{BET} = 0.8$ m^2/g) or a high specific surface area calcite, Calofort U, $S_{BET} = 21$ m^2/g). Specific surface area is measured by nitrogen adsorption (BET, Micromeritics Gemini 2375).

Solution pH and free calcium are recorded with ion selective electrodes (pH: Orion 8115BN, Ca: Orion 9700BN). The high surface area powder was also used for zeta potential measurements in solutions of precise composition and compared with the predicted calculations. The zeta potential measurements were made using electroacoustics performed on a Colloidal Dynamics AcoustoSizer II.

For dilute colloids in concentrated electrolytes, for small zeta potential or for large particles (inertia impedes their motion) the background signal can be significant. Therefore, background subtraction is made on the measured results. The background is given by the electrolyte solution after the particles have been removed by centrifugation.

2.2. Methods

2.2.1. Theoretical methods

The details of the thermodynamic solubility model, the assumed reaction pathway, surface potential calculations, the calculation of interfacial energy and the link between calcium carbonate

solubility and particle size are given in detail in supplementary material (S1). Here we will describe qualitatively the approach, the use and outcome of the theoretical approaches.

The solubility calculations allow us to take into account a large number of chemical equilibria between ions and complexes in solution and possible solid phases depending on the concentrations of the solution species. The approach is based on a method developed by Rubattel and Lemaître [4] and Vereecke and Lemâitre [5] and calculates activity coefficients to convert the thermodynamic activities into concentrations which can be measured experimentally (S1.1). The test case use in this study is the precipitation of calcium carbonate from aqueous calcium nitrate and potassium carbonate solutions. In this system 19 different equilibria are considered. This allows us to calculate the species in solution and hence the pH of the system as a function of solution composition which varies as we move from a supersaturated solution just after mixing 0.02 M solutions towards an equilibrium with the precipitated solid phase. The pH can be monitored experimentally and thus related to a degree of reaction (ξ) (S1.2). This is computationally carried out for a series of supersaturations and thus allows us to follow a reaction pathway with information on the species in solution and the precipitated solid phases predicted by the thermodynamic calculations.

We have also used Nerst's law to predict the surface potential Φ_0 of calcium carbonate which is related to the activity of the potential determining ions which in this case are Ca^{2+} and CO_3^{2-}. This surface potential will vary as the species in solution varies and can be related to the experimentally measureable zeta potential (S1.3).

When precipitation takes place stable nuclei are created after an induction period and then grow to form crystals which may or may not agglomerate depending on their colloidal stability. These nuclei are often very small a few nm and their solubility is different to a bulk crystal as expressed by Kelvin's law (S1.4). Thus in our model we can take into account changes in solubility and thus solution composition as a function of the particle size. A key factor in the use of Kevin's Law is the solution-solid interfacial energy, γ. This a difficult parameter to evaluate experimentally during the dynamic situation of precipitation and crystal growth and according Mersmann [1] it varies during a precipitation reaction. Mersmann developed an approach to calculate γ_0 from the concentration of ions in solution [1]. However the different species in solution (Table S1) were not taken into account in this approach and we have modified the approach to rectify this situation (S1.5).

Thus our theoretical model allows us to predict the change in pH, surface charge, quantity of solid phase precipitated as we decrease the supersaturation step-by-step. This can then be related to experimentally measurable quantities such as calcium activity using specific electrode, pH, zeta potential and the precipitated phase (for example by X-ray powder diffraction).

2.2.2. Zeta potential measurements

For validation of the various approaches used in the above sections zeta potential measurements on calcite powders under well controlled conditions have been made. Samples of the Calofort calcite, 5.89 wt%, were prepared by mixing 11.78 g $CaCO_3$ in 188.22 g of different electrolyte solutions, with compositions as shown in Table 2b. The samples were treated by ultrasonic-horn for 15 min (400 watts, 20 MHz) and magnetically stirred for 15 min. Zeta potential measurements were then performed on the AcoustoSizer II 30 min after the initial mixing. The measurements were repeated after 72 h (samples with closed lids to exclude absorption of atmospheric CO_2) to ensure that equilibrium with respect to the species in solution had been achieved. Before the 72 h measurements, the samples were again treated by UH15 and stirred for 15 min.

3. Results and discussion

3.1. Solubility and surface potential

The application of the Nernst law for the evaluation of ζ potential has been evaluated by comparing calculated values with well documented literature data [18,19] as well as our electroacoustic zeta potential measurements. Although the calculation of zeta potentials are fraught with uncertainties, for the particles sizes (μm) and ionic concentrations discussed below the Debye length will always be small (a few nm) and Smoluchowski's approximation has been used for the electroacoustics and the electrophoretic measurements in [19]. Also at the relatively low ζ potentials measured (<25 mV) the approximation is very good. The streaming ζ potentials measured in [18] are estimated from streaming potential measurements (using the Helmholtz equation) and from a large number of measurements the error in the ζ potential was reported to be a maximum of 10%. Unfortunately, temperature measurements are not reported but comparison between calculated and measured pH (measured pH = 9.00—9.14, calculated pH = 9.08) shows a good correlation when considering measurements carried out at 25 °C. Comparison of measured and our calculated values show a very good agreement when the hydrodynamic parameter ψ is adjusted to 0.45 and considering the counter ions parameter C_0 equal to 0 (Fig. 2). The experimental values were measured in the presence of some counter ions ($NaCl = 510^{-3}$ M, $NaHCO_3 = 10^{-3}$ M) and pH adjustments were carried out by adding calcium hydroxide (triangle, Fig. 1) or carbon dioxide (diamonds, Fig. 1).

In Fig. 2, not only do the calculated values agree well with measured ones, but also the trend is correctly described by the calculation. This agreement indicates first that our calculation of the potential of zero charge (Table 1) seems to be correct; second that our solubility data are adequately defined so that our calculation of the potential determining ion activities is accurate.

Thompson et al. [18] observed a hysteresis effect by a forward/reverse titration of the same system as described in Fig. 2 (dotted lines and symbols). Calculations of the ζ potential predict that small variations of the ionic strength in these conditions should not change the ζ potential to such a degree. To explain this hysteresis, Thompson et al assumed a surface modification of the calcium carbonate powder, by a secondary aragonite precipitation on the surface of the calcite powder in the streaming potential apparatus (a packed bed). Calculation of the first hypothesis using our approach cannot explain the amplitude of the hysteresis (Fig. 2A). We have also made calculations according to a second hypothesis, where the system does not reach an equilibrated state during the acid titration and the calcium concentration remains constant in solution. The system becomes supersaturated but time is too short

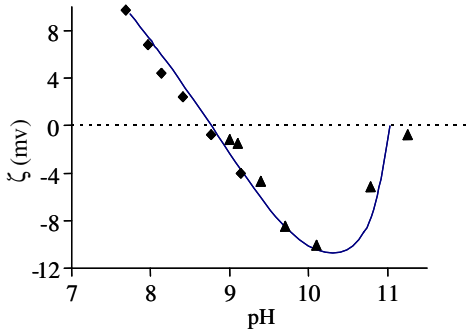

Fig. 1. Comparison between the measured ζ potential (diamonds and triangles) (18, Fig. 4) with the calculated ζ potential from Eq. 8 ($\psi = 0.45$ et $C_0 = 0$) (line).

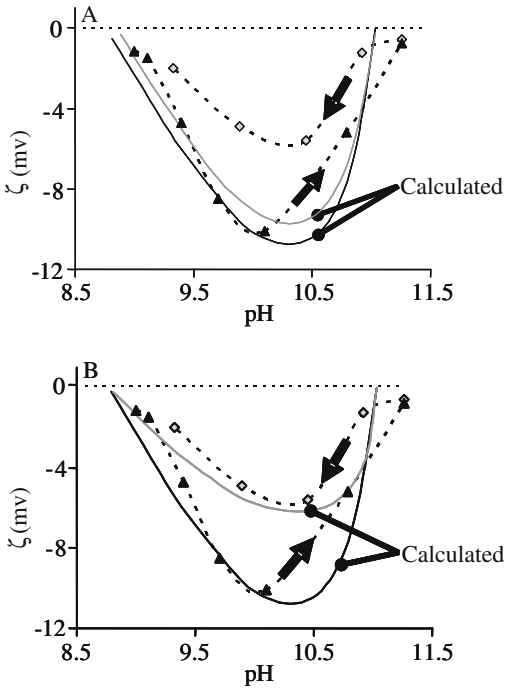

Fig. 2. Simulation using solubility calculations for different hypotheses to explain the hysteresis effect on the ζ potential when using a forward/reverse titration. pH adjusted by adding first $Ca(OH)_2$ (triangles) then H_2CO_3 (diamond). (A) Aragonite formation on the surface of calcite crystals, the equilibrium is consequently achieved with this aragonite. (B) During the reverse titration, the system does not reach an equilibrium state and the calcium concentration remains constant. The system is also supersaturated.

Table 1
(a) Calcium and carbonate potentials at the isoelectric point calculated according to the hypothesis of crystal equilibrium state in pure water and (b) zeta potential measurements (electroacoustics[a]) carried out in the presence of different electrolyte with the Calofort high purity calcite (25 °C).

T (C°)	Phase	pCa_{pcz}	pCO_{3pcz}	pH
(a)				
25	Calcite	3.97	4.51	9.90
25	Aragonite	3.92	4.42	9.95
	30 (min)		72 (h)	
Electrolyte	pH	ζ (mV)	pH	ζ (mV)
(b)				
0.004M K_2CO_3	10.49	−7.4	10.55	−7.4
0.004M Na_2CO_3	10.49	−7.1	11.53	−7.5
0.004M Li_2CO_3	10.53	−8.2	10.47	−7.3
0.04M K_2CO_3	11.14	−11.3	11.23	−11.0
0.04M Na_2CO_3	11.00	−10.9	11.03	−10.6
0.04M Li_2CO_3	11.03	−13.4	11.10	−13.6

[a] Background correction was made on solutions after removal of powder by centrifugation (zeta from two measurements ± 0.2 mV).

for calcite precipitation to occur. This hypothesis correlates better with the experimental data (Fig. 2B).

The hypothesis of the non-equilibrium state during the reverse titration seems reasonable when we consider the supersaturation and induction times for aragonite. In fact the supersaturation created during the acidification of the solution is low ($S_{max} = 2.9$) and the induction time would therefore be long (>8 h according to [20]). Thus a 15 h wait between each measurement made by Thompson et al. may not be long enough to reach the real equilibrium state assumed in the calculations for Fig. 2A.

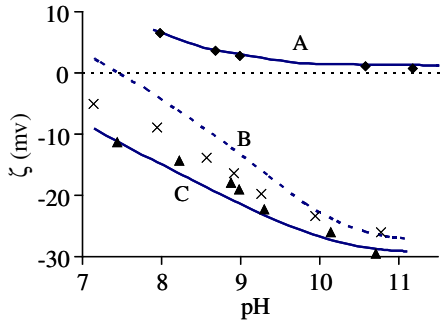

Fig. 3. Comparison between calculated ζ potential (line) and experimental values (symbols) (18, Fig. 3). A (diamond): $CaCl_2 = 5 \times 10^{-4}$ M, $C_0 = -6$; B (cross): $NaCl = 5 \times 10^{-3}$ M, $C_0 = -14$; C (triangle): $NaCl = 5 \times 10^{-3}$ M, $NaHCO_3 = 10^{-3}$ M, $C_0 = -26$. The pH is first adjusted by adding NaOH and the titration starts by adding HCl. Full lines correspond to the equilibrium state at each pH. The ψ parameter is 0.45.

For the same calcite system when the pH is adjusted by adding sodium hydroxide or hydrochloric acid the zeta potential measured is different [18]. For the modelling this means the C_0 constant changes because of a possible adsorption of hydroxide ions or protons at the surface (Eq. (S1.9)) and thus has to be adjusted. The ψ constant is kept at the same value (0.45) as the hydrodynamic conditions in the streaming potential measurement have not changed [18]. The calculated values fit the experimental data well over the whole pH range for two cases with just an adjustment of C_0 (Fig. 3). The case with the discrepancy may be caused by a non-equilibrium state for this measurement as discussed in previous section.

We have also compared the ζ potential measurements with experimental data using electrophoresis at 25 °C [19]. In this case also, the calculated ζ potential trends correspond well with the experimental trends using the same ψ parameter (0.45). To obtain a good fit, only the C_0 parameter has to be adjusted (Fig. 4).

The comparisons carried out between the measured ζ potential and the calculated value (Eq. (S1.9)) shows that the joint use of Nernst equation and solubility calculations is a good way to predict the surface charge modifications of calcite induced by the surrounding medium. The hydrodynamic parameter ψ seems to be able to be treated as a constant even when using different measurement methods. Only the chemical adsorption parameter, C_0, shows significant changes according to measurement conditions. This variation reflects the difference between the surface and Stern layer potentials (Φ_0 and the Φ_s, S1.3) which may be influenced by the adsorption of non-specific ions in the Stern layer (for example: Cl^-, OH^-, H^+). To try and clarify this, a series of zeta potential

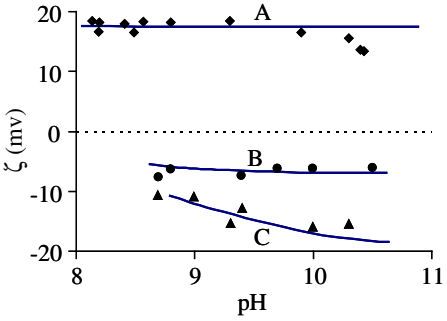

Fig. 4. Comparison between the experimental ζ potential (points) (19, Fig. 1), and the calculated values (line). A (diamond): $CaCl_2 = 10^{-2}$ M, $C_0 = -5$; B (circle): $CaCl_2 = 10^{-3}$ M, $C_0 = -16$; C (triangle): NaCl only, $C_0 = -16$. In all cases, $I = 0.03$ M, and pH is adjusted by NaOH/HCl; $\psi = 0.45$.

Table 2
Values of interfacial energies of different calcium carbonate polymorphs in pure water.

Polymorph	γ_{calc} Eq. (S1.19) 10^{-3} (N/m)	$\gamma_{exp}10^{-3}$ (N/m)	Refs.	$\gamma_{expother}10^{-3}$ (N/m)	Refs.
Calcite	142	98	[21]	19.5–280	[28,29]
Aragonite	149	150	[21]	150	[29]
Vaterite	133	34	[27]	6.8–108	[21,29,30]

measurements with the carbonates of K, Na and Li were carried at two different concentrations (Table 1 (b)). The ζ potential results are shown in Table 1b where little effect of the cation is seen giving similar zeta potentials from K^+ to Na^+ to Li^+ at 0.004 M.

For the higher concentrations the smallest ion Li^+ does show an increase in the zeta potential. This possible effect of non-specific ions supports the argument for the effect that such ions can have on the C_0 value for higher ionic concentrations as discussed above. The exact relationship between the concentrations of these ions and C_0 is not yet clear and needs further investigation which is beyond the scope of the current investigation.

3.2. Solubility and interfacial energy

Direct determination of interfacial energy for powders is very difficult. Conventional contact angle measurements are not suitable for powdered materials therefore other methods, usually nucleation experiments [3,21], are used. However, the values reported in literature vary widely. For example, calcite–water interfacial energies reported in the literature vary between 19.5×10^{-3} N/m and 280×10^{-3} N/m [21]; according to these authors, the highest values are probably from an incorrect interpretation of the results whereas the lowest results are probably due to heterogeneous nucleation caused by foreign surfaces in the reactor (e.g. dust or reactor walls) and not the homogenous nucleation assumed in the theoretical description used. A comparison between calculated values (Eq. (S1.19)) and some experimental data of the interfacial energy values are shown in Table 2, for calcite, aragonite and vaterite.

Interfacial energies calculated with the Mersmann–Eble [1,22] approach (Eq. (S1.19)) are usually higher than those reported in the literature. This can be explained by several different considerations:

First, according to Eq. (S1.19), the interfacial energy of a precipitating powder changes with reaction progress. For example, taking into account an initial concentration of the reactant at 0.02 M of calcium nitrate and sodium carbonate, then the calcite–water interfacial energy is 92×10^{-3} N/m at the beginning of the reaction and 135×10^{-3} N/m at the end of the reaction. Therefore, the calculated interfacial energy according to the nucleation theory is either the value at the beginning of the reaction, or an average value between some compositions of the solution thereafter. With a detailed knowledge of the experimental conditions, Eq. (S1.19) should give a variable but well defined result. Unfortunately, most experimental data are not given in enough detail in the literature to do this, often only graphical representations are reported.

Second, the precipitation mechanism could explain experimental interfacial energy values lower than those calculated. In fact, if some hydrated carbonate phase (such as ikaite) is a precipitated precursor of the anhydrous calcium carbonate, the interfacial energy determined with the nucleation method is that of the hydrated phase, which is lower than for the anhydrous phase [22–24].

Third, if some heterogeneous nucleation takes place during the precipitation experiment, experimental values of the interfacial energy will be lower than those calculated for the crystal. All three reasons indicate that the determination of the interfacial energy with precipitation experiments is difficult to interpret correctly and do not necessarily reflect the intrinsic interfacial energy of the crystal. Another possibility is the specific adsorption of counter ions during precipitation – for the systems discussed below several authors [18,19] have shown that only Ca^{2+} and CO_3^{2-} ions are potential determining and thus the use of the Nernst equation and its implicit assumptions can be used (at least after the early stages of the precipitation where a hydrated phase may be present). Taking into account all these limitations, the calculated interfacial energies, Table 2, seem reasonable. To verify more accurately the use of Eq. (S1.19), a number of experiments described in the following paragraph were carried out.

4. Experimental verification of interfacial energy calculations

Solubility measurements were carried out in order to verify our approach to the interfacial energy calculations by comparison with the Kelvin equation (Eq. (S1.16)) calcium carbonate powder (Fluka, 21060) was equilibrated in 0.0403 M or 0.00403 M potassium carbonate aqueous solutions. These concentrations cover the range of ionic concentrations for the zeta potential experimental studies [18,19] and the precipitation experiments discussed in the following section. These solutions were used as standards for electrode calibration (Calibs 1 and 2, Table 3) because of the large size of the primary crystals ($S_{BET} = 0.8\ m^2/g$). Measurements were then made on a solution containing Calofort U calcium carbonate powder equilibrated under the same conditions as for the electrode calibration. The Calofort U powder contains nano-particles as indicated by the specific surface area measurement ($21\ m^2/g$). Differences in calcium activities between the calibration powder (Fluka) and the measured powder (Calofort U) can be explained by the size difference in primary crystallites changing consequently the solubility (Kelvin law, Eq. (S1.16)). As the specific surface area of the Calofort U powder is well-known, the only adjustable parameter in the Kelvin equation is the interfacial energy. Comparison be-

Table 3
Interfacial energy of calcite powder (Calofort U) obtained from the Kelvin equation and solubility measurements (Eq. (S1.16)) and from the mathematical calculation (Eq. [19]).

Experience	(CO_3^{2-})	pH_{meas}	pH_{calc}	$(Ca^{2+})_{meas}10^{-7}$ (M)[a]	$S_{BETCalorfort}$ (m^2/g)	γ Eq. (S1.16) 10^{-3} (N/m)	γ Eq. (S1.19) 10^{-3} (N/m)
Calib 1	0.0403	11.20	11.20	3.53 ± 0.03			
Calib 2	0.00403	10.87	10.87	17.0 ± 0.5			
Exp 1	0.0403	11.17	11.23	3.71–3.77	21	39–53	41
Exp 2	0.00403	10.83	10.89	19.2–20.5	21	107–164	118

[a] From 5–10 measurements.

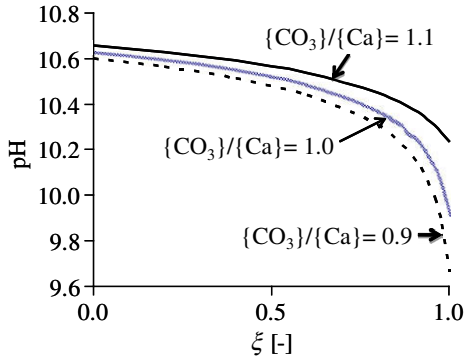

Fig. 5. pH evolution versus precipitation progress for different $\{CO_3\}/\{Ca\}$ ratios.

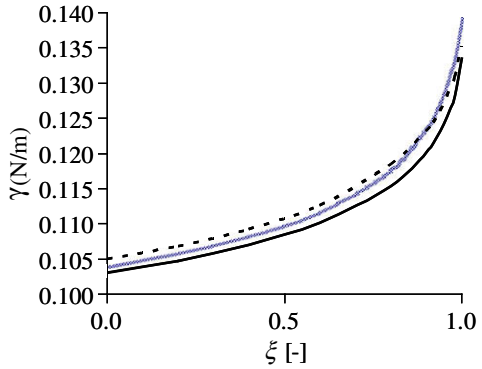

Fig. 7. Interfacial energy evolution during the precipitation of calcite in the considered experiments.

tween experimental and calculated interfacial energy (Eq. (S1.19)) is reported in (Table 3).

Comparison between the calculated interfacial energy with the modified Mersmann–Eble equation (Eq. (S1.19)) and the Kelvin equation (Eq. (S1.16)) shows very good agreement. This agreement highlights the importance of combining interfacial energy and solubility calculations. This agreement confirms also the internal consistency of our calculation, including the surface potential calculations.

5. Prediction of reaction pathway

The validity of different equations used to derive surface potentials and interfacial energies of powders from solubility calculation have been presented in previous sections. The next step is to apply these calculations to simulate possible reaction pathways of precipitating systems; the solubility calculations provide full knowledge of solution composition during the precipitation progress. We shall consider as an example the theoretical case of initial solution composition variation close to the equimolar point. The considered reaction is calcite precipitation using calcium nitrate and sodium carbonate as reactants at 0.004 M with either perfect stoichiometry or 10% excess of carbonate or calcium ions. In such conditions, the induction time for nucleation should be 24 s and the total completion of the reaction (precipitated calcium carbonate) should be less than 10 min according to experimental data [20]. By using the thermodynamic solubility calculations the pH behaviour during the reaction can be accurately described (Fig. 5). The final pH value will be directly related to the initial stoichiometry of the reactants. Small changes in the calcium to carbonate ratio also influences significantly the surface potential of the powder which has also been computed for the above cases (Fig. 6).

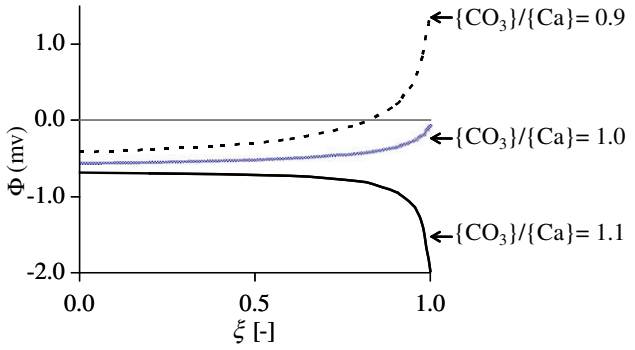

Fig. 6. Surface potential of the calcite powder during the reaction progress.

The divergence of the final surface potential can influence significantly the possible agglomeration of the precipitating particles during the reaction. In fact, if 10% excess of carbonate is present in solution, the absolute value of surface potential increases monotonically which can increase the colloidal stability of precipitating particles. In the stoichiometric case, the surface potential tends towards zero, which could promote an agglomeration process. For the 10% excess of calcium, we pass the potential of zero charge which would lead to enhanced kinetics of agglomeration at a higher residual supersaturation creating hard agglomerates [25]. The use of this new approach can therefore help to better understand precipitation reactions and the particle formation mechanism that can be tailored as a function of reaction progress. For these conditions the interfacial energy also changes during the reaction (Fig. 7).

For the interfacial energy, the initial concentration of the solution is not so important. Nevertheless, the interfacial energy increases with the reaction progress. If during the reaction, a phase transformation occurs, then the increase in the surface energy becomes more important. This increase in surface energy would also promote possible agglomeration process or some other surface reaction at the end of the reaction in order to minimise the total energy of the system. Attempts to follow experimentally the above behaviour with pure solutions (e.g. agglomeration as a function of time) proved to be impossible because of the speed of the reaction, even using synchrotron radiation at ELLETRA (Italy) at the necessary concentration to detect particles the initial nucleation and growth process were too quick. Further work using cryogenic Transmission Electron Microscopy (cryo-TEM) were also pursued to try and support our predicted mechanisms but without seeds or polymeric additives it was very difficult to control the precipitated phase to be either pure calcite or pure vaterite [26] and further experimental work beyond the scope of the current manuscript is needed.

6. Summary

Solubility calculations based on the thermodynamic equilibrium of the species in solution give exciting possibilities to help clarify and predict the outcome of precipitation reactions. Not only can the real effective supersaturation of precipitating solutions be obtained using these solubility calculations, but also simulations of reactions pathways, which can then be related to easily measureable experimental parameters such as pH. Solubility calculations can also be extended to interfacial energy or a particle size in equilibrium with a solution determined only using solubility measurements. Comparison with experimental values and calculated values shows a good agreement using different approaches. These

extended approaches can be applied to calculate surface charge changes or interfacial energy evolution during precipitation reactions for ionic crystals where the potential determining ions are known, by the application of Nernst's law. All these applications have been illustrated with calcite precipitation and they open new avenues to highlight and predict the evolution of precipitation reactions.

Acknowledgments

This research was conducted during the 5th European Framework (programme Growth; project SFTR No. CE: G5RD-CT99-0123) and financially supported by the Swiss OFES (No. 99.0449-1).

The authors would also like to thank Mr. A. Schuler for the electroacoustics measurements.

Appendix A. Supplementary material

Supplementary data associated with this article can be found, in the online version, at doi:10.1016/j.jcis.2009.09.005.

References

[1] A. Mersmann, J. Cryst. Growth. 102 (1990) 841.
[2] A.E. Nielsen, J. Cryst. Growth. 67 (1984) 28.
[3] A.E. Nielsen, O. Söhnel, J. Cryst. Growth. 11 (1979) 233.
[4] S. Rubattel, J. Lemaître, P. Bowen, T.A. Ring, J. Cryst. Growth. 135 (1994) 135.
[5] G. Vereecke, J. Lemaître, J. Cryst. Growth. 104 (1990) 820.
[6] L.N. Plummer, E. Busenberg, Geochim. Cosmochim. Acta 46 (1982) 1011.
[7] L.N. Plummer, E. Busenberg, Geochim. Cosmochim. Acta 51 (1987) 1393.
[8] J.Y. Gal, J.C. Bollinger, H. Tolosa, N. Gache, Talanta 43 (1996) 1497.
[9] L. Brecevic, A.E. Nielsen, J. Cryst. Growth. 98 (1989) 504.
[10] J.R. Clarkson, T.J. Price, C.J. Adams, J. Chem. Soc., Faraday Trans. 88 (2) (1992) 243.
[11] N. Nassrallah-Aboukais, A. Boughriet, J. Laureyns, L. Gengembre, A. Aboukais, Chem. Mater. 11 (1999) 44.
[12] N. Vdovic, D. Kralj, Colloid Surf.: A. Physicochem. Eng. Aspects 161 (2000) 499.
[13] W.D. Bischoff, F.T. Mackenzie, F.C. Bishop, Geochim. Cosmochim. Acta 51 (1987) 1413.
[14] J.A. Davis, C.C. Fuller, A.D. Cook, Geochim. Cosmochim. Acta 51 (1987) 1477.
[15] E.K. Giannimaras, P.G. Koutsoukos, Langmuir 4 (1998) 855.
[16] P.G. Koutsoukos, C.G. Kontoyannis, J. Chem. Soc., Faraday Trans. I 80 (1984) 1181.
[17] M.M. Reddy, J. Cryst. Growth. 41 (1977) 287.
[18] D.W. Thompson, P.G. Pownall, J. Colloid Interface Sci. 131 (1) (1989) 74.
[19] D.S. Cicerone, A.E. Regazzoni, M.A. Belsa, J. Colloid Interface Sci. 154 (2) (1992) 423.
[20] W.-C. Chien, C.Y. Tai, J.-P. Hsu, J. Chem. Phys. 111 (6) (1999) 2657.
[21] O. Söhnel, J.W. Mullin, J. Cryst. Growth. 60 (1982) 239.
[22] A. Eble, PhD Thesis, München, 1–50, 2000.
[23] H. Cölfen, L. Qui, Chem. Eur. J. 7 (1) (2001) 106.
[24] J. Rieger, J. Thieme, C. Schmidt, Langmuir 16 (2000) 8300.
[25] M.J. Hounslow, A.S. Bramley, W.R. Paterson, J. Colloid Interface Sci. 203 (1998) 383.
[26] M. Donnet, P. Bowen, N. Jongen, J. Lemaître, H. Hofmann, Langmuir 21 (2005) 100–108.
[27] D. Krajl, L. Brecevic, A.E. Nielsen, J. Cryst. Growth 104 (1990) 793.
[28] L. Holysz, E. Chibowski, J. Colloid Interface Sci. 164 (1994) 245.
[29] J. Gomez-Morales, J. Torrent-Burgues, R. Rodriguez-Clemente, J. Cryst. Growth. 169 (1996) 331.
[30] F. Manoli, E. Dalas, J. Cryst. Growth 217 (2000) 416.